J. Membrane Biol. 170, 103–119 (1999)

The Journal of
Membrane
Biology

Activation Kinetics of the K^+ Outward Rectifying Conductance (KORC) in Xylem Parenchyma Cells from Barley Roots

L.H. Wegner*, A.H. De Boer

Faculty of Biology, Department of Molecular Genetics, Section of Plant Physiology, Vrije Universiteit Amsterdam, De Boelelaan 1087, 1081HV Amsterdam, The Netherlands

Received: 20 November 1998/Revised: 1 April 1999

Abstract. The activation kinetics of outward currents in protoplasts from barley root xylem parenchyma was investigated using the patch-clamp technique. The K^+ outward rectifying conductance (KORC), providing the main pathway for K^+ transport to the xylem, could be described in terms of a Hodgkin-Huxley model with four independent gates. Gating of KORC depended on voltage and the external K^+ concentration. An increase in the external K^+ concentration resulted in a shift in the voltage dependence of gating. This could be explained by a K^+ dependence of the rate constant β for channel closure, indicating binding of K^+ to a regulatory site exposed to the bath. Occasionally, KORC was observed to inactivate; this inactivation occurred and vanished spontaneously. In some of the whole cell and excised patch recordings, a stepwise increase in outward current was observed upon a depolarizing voltage pulse, indicating that several populations of 'sleepy' channels existed in the plasma membrane that activated with a certain lag time. It is discussed whether this observation can be explained by a putative subunit, which retards channel activation, or by a scheme of cooperative gating. A quantitative description of outward rectifying K^+ channels in xylem parenchyma cells is a major step forward towards a mathematical model of salt transport into the xylem.

Key words: Plant ion channel — Hodgkin-Huxley formalism — Cooperative gating — K^+ dependent gating

**Present address:* Am Lehrstuhl für Biotechnologie, Universität Würzburg, Biozentrum, Am Hubland, D-97074 Würzburg, Germany

Correspondence to: L.H. Wegner

Introduction

Release of K^+ by xylem parenchyma cells in the root occurs via outwardly rectifying K^+ channels (KORCs) in the plasma membrane of these cells (Wegner & Raschke, 1994; Roberts & Tester, 1995, 1997; Wegner & De Boer, 1997). The central role of these channels for the translocation of potassium from the root to the shoot was first demonstrated by Wegner and De Boer (1997). By perfusing the stele of young barley seedlings with the K^+ channel blocker TEA, accumulation of K^+ in the shoot was completely inhibited. Further evidence for K^+ channels serving as major pathways for K^+ release to the xylem sap came from the recent report by Gaymard et al. (1998) on the cloning of a K^+ outward rectifier exclusively expressed in root stelar cells of *Arabidopsis* (SKOR, stelar K^+ outward rectifier). A highly homologous sequence with a similar expression pattern has also been found in maize, (C. Alcon and H. Sentenac, *personal communication*), suggesting that SKOR may be common to dicots and monocots. In knockout mutants of *Arabidopsis* lacking SKOR, shoot K^+ content and xylem sap concentration of K^+ were reduced significantly. The electrophysiological properties of SKOR were studied by heterologous expression in *Xenopus* oocytes. Several lines of evidence indicate that the properties of SKOR are identical with those of KORC (Wegner & De Boer, 1997; Gaymard et al., 1998): (i) The activation potential of the channel shifts with a change in the external K^+ concentration, (ii) whole cell currents activate with sigmoidal kinetics upon a stepwise depolarization of the membrane, (iii) besides K^+, the channel translocates Ca^{2+}, (iv) the expression of SKOR is downregulated by the phytohormone ABA, leading to a decrease of the outward K^+ currents in stelar cells when plants were pretreated with ABA (Roberts, 1998).

In this report, we focus on the gating properties of KORC (SKOR) in xylem parenchyma cells from barley roots. A quantitative analysis of gating will serve several purposes: It will provide a basis for the comparison of patch clamp and oocyte data, revealing in which way the "natural environment" of the channel alters its properties. Furthermore, knowledge of the gating properties of KORC is required to calculate K^+ efflux across the plasma membrane of root stelar cells. From a physiological point of view, the dependence of KORC gating on the external potassium concentration is of special interest, since Wegner & De Boer (1997) have proposed that the apoplastic K^+ concentration in the root, as influenced by K^+ recirculated via the phloem, is a key factor in the regulation of K^+ transport from the root to the shoot (*see also* Drew, Webb & Saker, 1990).

Kinetics of the KORC will be analysed in terms of the Hodgkin-Huxley model of channel gating (Hodgkin & Huxley, 1952) that has also been applied successfully to plant K^+ channels (Schroeder, 1989; van Duijn, 1993; Fairley-Grenot & Assmann, 1993; Roberts & Tester, 1995; Vogelzang & Prins, 1995) and anion channels (Kolb, Marten & Hedrich, 1995).

Materials and Methods

Growth of barley and protoplast preparation were performed as described in detail earlier (Wegner & Raschke, 1994; Wegner & De Boer, 1997). The experimental setup for patch clamping was as described by Wegner & De Boer (1997). Data reported here were recorded in the whole cell, outside-out and inside-out configuration.

Data Analysis

Data were filtered at 1 kHz and sampled at 3 kHz if not stated otherwise. For generation of pulse protocols and basic evaluation, the software package EPC (Cambridge Electronic Design, Cambridge, U.K.) was used on a PC (HP Vectra). For futher analysis, data were transferred to a Macintosh computer. For a mathematical description, data were fitted with the least square method using the Levenberg-Marquard algorithm. Fitting was done with the graphic program 'Kaleidagraph' (Abelbeck software, USA). Special data reduction for kinetic analysis was only performed in a few cases as indicated in the figure legends.

Solutions

For whole cell recordings, standard solutions contained: *Bath* 1, 10, 30 or 100 mM KCl, 2 mM $MgCl_2$, 1 mM $CaCl_2$, 10 mM HEPES (pH 5.8 adjusted with BTP); *pipette* 120 mM KCl, 10 mM EGTA, 4.42 mM $CaCl_2$, 2.27 mM $MgCl_2$, 2 mM MgATP, 10 mM TRIS or BTP (pH 7.2 adjusted with MES; free Ca^{2+} = 150 nM, free Mg^{2+} = 2 mM). If solutions were composed differently, this is indicated in the figure legends. All solutions used were adjusted to a final osmolality of 500 mosmol/kg by adding an appropriate amount of mannitol. Part of the observations reported here on the kinetics of outward currents were made in the course of studies on the selectivity and regulation of the channels. As a consequence, the composition of the solutions varies with respect to the counterion for K^+ (Cl^- or glutamate) and the cytosolic Ca^{2+} concentration (150 nM or 1 μM). Within limits of accuracy, gating properties of KORC remained unaffected by these modifications of the experimental conditions.

Results

Gating properties of ion channels can be extracted from current relaxation upon a stepwise change in the clamped voltage by a mathematical analysis of the time course (Hille, 1992). The most frequently applied formalism to describe these current changes is that designed by Hodgkin & Huxley (1952) to model depolarization-activated Na^+ and K^+ channels in the squid axon (*see* Introduction). The mathematical expressions derived by Hodgkin & Huxley have been applied to various types of channels, including those in plant tissue. According to the model, current activation is described by the relation (Schroeder, 1989; van Duijn, 1993):

$$I(t) = I_{leak} + I(1 - \exp(-t/\tau_{act}))^p \quad (1)$$

I_{leak} is the leak current, I is the steady-state current carried by the channel at a given voltage, τ_{act} is the time constant for activation and p is the number of independent gating particles. This equation holds if (almost) all gates are in the closed state at the prepulse potential. In the case of an outward rectifier it means that the membrane must be sufficiently hyperpolarized. Often however, the experimenter is forced to choose a more positive holding potential to minimize background conductances and to maintain a stable patch. For xylem parenchyma protoplasts, a holding potential of about −100 mV is most suitable. In this case, the correct kinetic parameters can be extracted from current relaxations by using an extended version of the Hodgkin-Huxley equation that takes into account the open probability per gate prior to the application of a voltage pulse (Armstrong, 1969; Wegner & De Boer, 1996):

$$I(t) = I_{leak} + G_{max}(U - E_{rev})\,[m_{start} + (m_\infty - m_{start})(1 - \exp(-t/\tau_{act}))]^p \quad (2)$$

with G_{max} being the maximal chord conductance, E_{rev} being the reversal potential of the channel, m_{start} being the 'activation variable' of an individual gate at the prepulse potential and m_∞ being the corresponding value after a new steady state has been reached.

Activation kinetics of KORC in xylem parenchyma protoplasts could most readily be studied with almost equal K^+ concentrations inside and outside the cell. By depolarizing excursions of the membrane voltage from a holding potential of −100 mV, clearly sigmoidal outward currents could be elicited as shown in Fig. 1 with 120 mM K^+ in the pipette and 100 mM K^+ in the bath. If p was included as a variable in the fit, values close to 4 were obtained (4.2 ± 0.2; data from three protoplasts. For

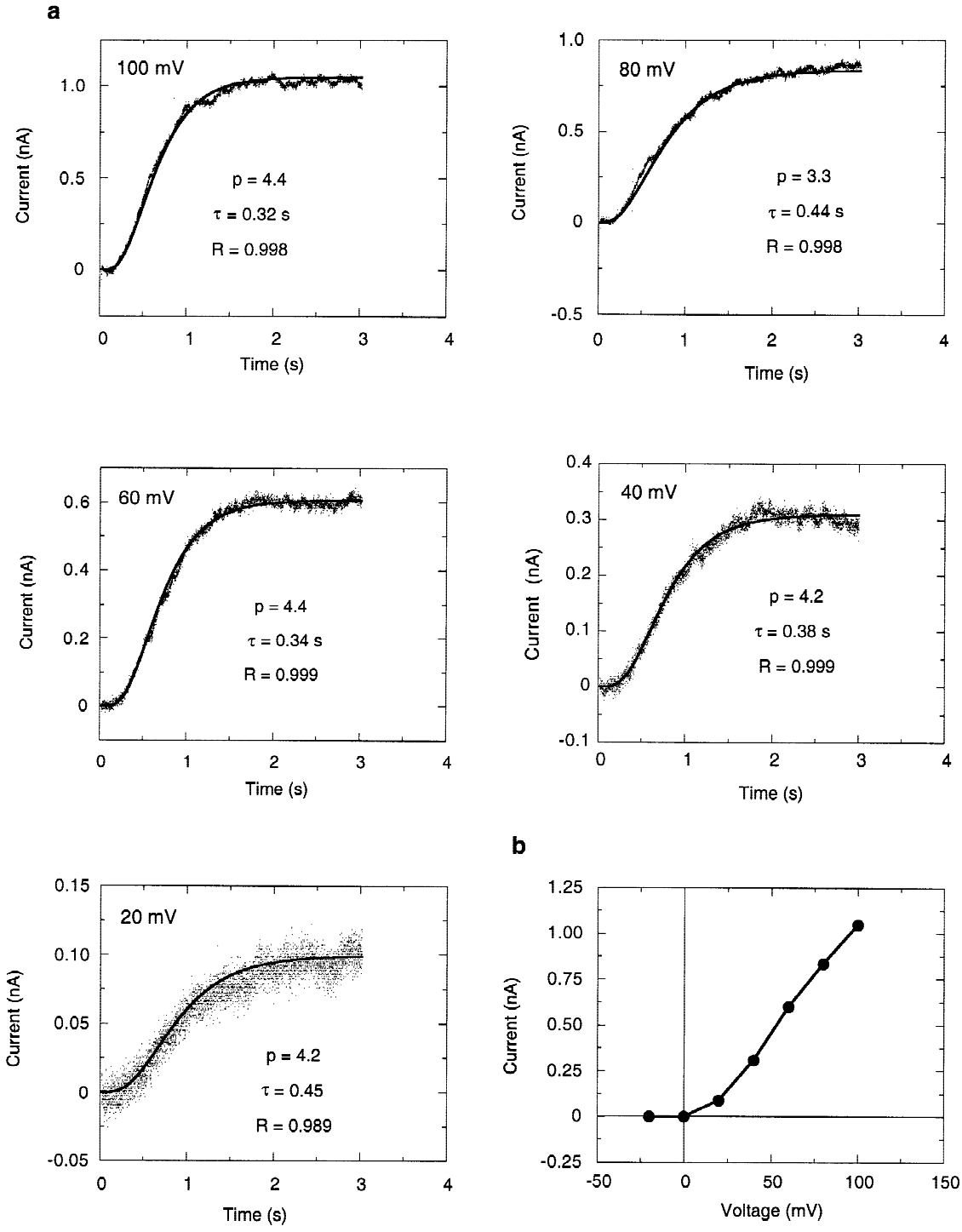

Fig. 1. Analysis of the kinetics of KORC activation with the Hodgkin-Huxley model. (*a*) Hodgkin-Huxley fit of KORC current activation (Eq. 1). From a holding potential of −100 mV, the membrane was depolarized to various potentials as indicated in the figures. Between successive pulses, the membrane was clamped to the holding potential for 10.75 sec. Standard solutions with 100 mM K^+ in the bath were used. The apparent number of gating particles (p), the time constant at which best fit was obtained (smooth line) and the regression coefficient are given below the traces. (*b*) The current level at m_∞, as obtained from the Hodgkin-Huxley fits shown in *a*, is plotted against the pulse potential.

each protoplast, *p* was determined for a range of command voltages by fitting individual current traces as shown in Fig. 1. Average values for *p* were calculated for three cells. The mean value ±SD was calculated from these cellular *p* values). It can be concluded that the sigmoidal kinetics of the channel could best be described with a model of four identical, independent gating particles per channel molecule. When K^+ in the bath was reduced, the activation potential of the KORC shifted to more negative voltages (Wegner & De Boer, 1997). As a consequence, the fraction of active gates at the holding potential (m_{start}) increased and the shape of the activation curve changed. In this case, the time course had to be fitted with Eq. 2. An example for the activation time course of KORC at 1 mM K^+ in the bath and 120 mM K^+ in the pipette is shown in Fig. 2*a*. The continuous line represents the best fit with Eq. 2. As a floating variable, *p* rendered a value of 3.7, in agreement with a model of four independent gating particles. Similar results were obtained for four other cells by applying a range of depolarizing voltage steps. The fraction of active gates, m_{start} and m_∞, were accessible from Boltzmann fits of the voltage dependence of the open probability. The ratio of open to closed gates can be expressed in terms of the energy change that the gates undergo when moving in the electrical field of the membrane:

$$\frac{m}{1-m} = \exp - \left(\frac{zF(U_{1/2} - U)}{RT} \right) \tag{3}$$

with *m* being the 'activation variable' of an individual gate, $U_{1/2}$ being the potential at which *m* is 0.5 (the 'midpoint potential') and *z* being the apparent minimal gating charge. *F*, *R* and *T* have their usual meaning. Transitions between the open and the closed state are expressed by the rate constants α and β according to

$$C \underset{\beta}{\overset{\alpha}{\rightleftarrows}} O$$

The open probability of a channel is then given by the equation (based on a model with four independent gating particles):

$$p_o(U) = m^4 = \frac{1}{\left[1 + \exp\left\{ (U_{1/2} - U) \frac{zF}{RT} \right\} \right]^4} \tag{4}$$

Note that the open probability is 0.0625 at the midpoint potential. The open probability at a certain conditioning voltage *U* can be derived from the tail current amplitude after repolarization to the holding potential:

$$p_o(U) = m^4 = \frac{I_{tail}(U)}{I_{tail,max}} \tag{5}$$

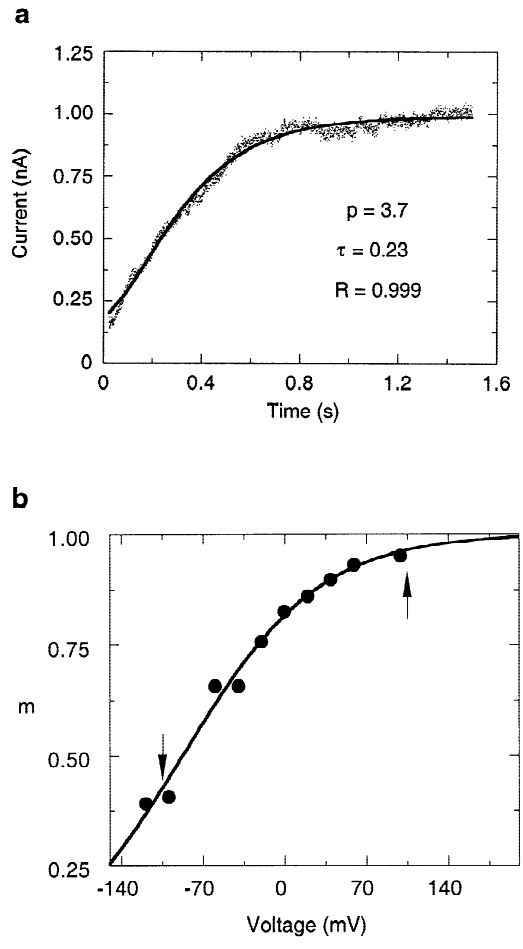

Fig. 2. A nonsigmoidal activation time course can be fitted with a Hodgkin-Huxley model provided that the voltage dependence of gating is known. (*a*) Analysis of the activation time course of KORC at 1 mM K^+ in the bath (standard solutions). Recorded data (noisy trace) were well represented by a Hodgkin-Huxley formalism (Eq. 2, continuous line). Optimal fit parameters are given in the figure. By Boltzmann fits (Eq. 4) to *m* (*b*), m_{start} (arrow downwards) and m_∞ (arrow upwards) could be determined. Data were calculated from the normalized chord conductance (Eq. 6) measured on the same protoplast that was probed in *a*.

However, tail currents were small or absent when K^+ in the bath was reduced to 1 mM. In this case, the open probability at this voltage was calculated according to

$$p_o(U) = m^4 = \frac{G_{K+}(U)}{G_{K+,max}} \tag{6}$$

where G_{K+}, is the chord conductance at the conditioning voltage *U* and G_{K+},*max* is the maximum chord conductance. For the same cell that was challenged with a depolarizing pulse in Fig. 2*a*, the increase of *m* with membrane depolarization is shown in Fig. 2*b*. Data were calculated from the steady-state current voltage curve of

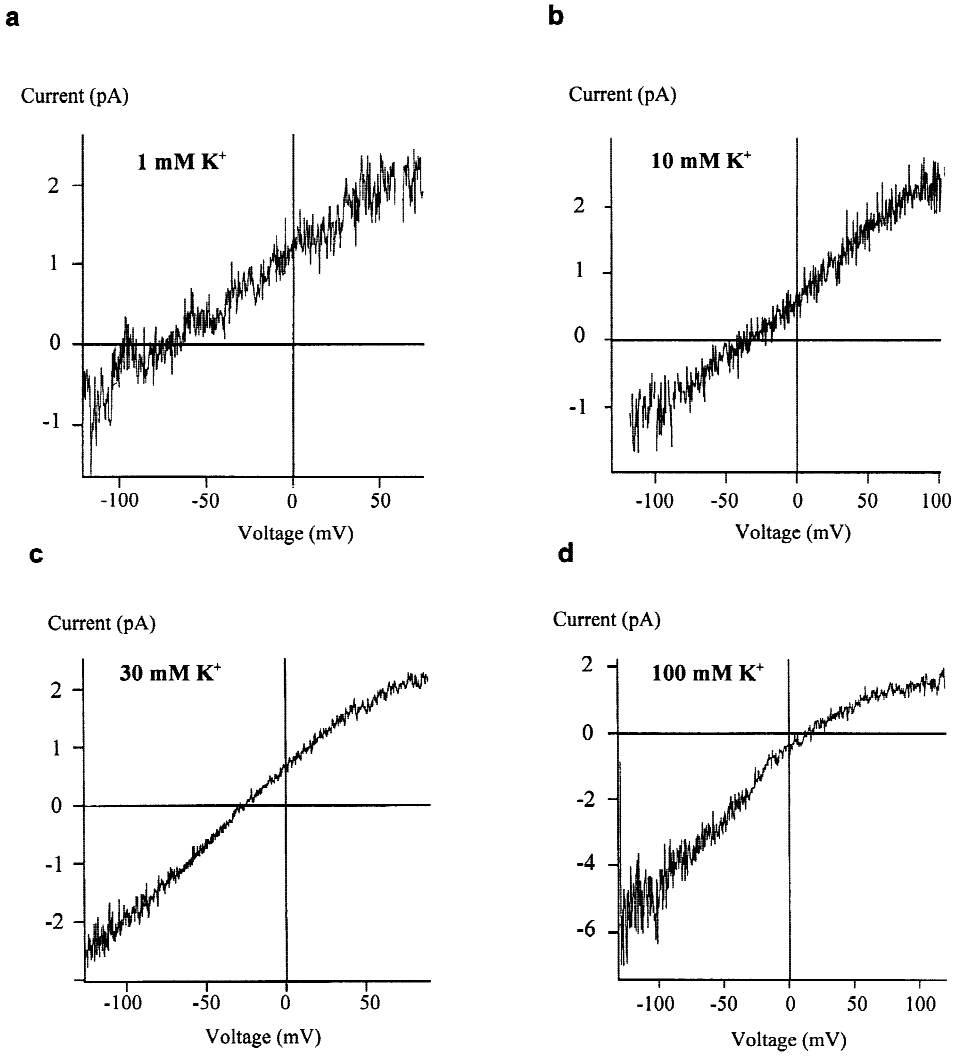

Fig. 3. Open channel ramps reflecting the current-voltage curves of KORC at different K^+ concentrations at the apoplastic (external) side of the membrane, as indicated in each figure. The cytoplasmic concentration was 120 mM. The traces shown are the mean of several scans; before the average was formed, leak subtraction was performed and closing events that occurred during a scan were removed. (*a*) Outside out patch, mean of 3 single channel scans. From a holding potential of 50 mV, voltage was lowered continuously to −150 mV in 250 msec. Time interval between scans: 3.25 sec. Standard solutions, but 120 mM K-glutamate in the pipette instead of KCl. (*b*) Inside out patch; mean of 5 single channel scans. From a holding potential of 70 mV, voltage was first clamped to 120 mV for 50 sec and then decreased to −130 mV in 300 msec. Time interval between ramps: 7.54 sec. *Pipette:* Standard bath solution with 120 mM K-glutamate. *Bath:* Standard pipette solution with 10 mM KCl in the bath. (*c*) Inside-out patch, mean of 16 single channel scans. From a holding potential of 70 mV, the patch was first stepped to 90 mV for 50 msec, followed by a voltage ramp to −130 mV in 200 msec. Between individual ramps, the voltage was clamped to the holding potential for 2.5 sec. Solutions as given for *b*, with the exception that the pipette solutions contained 30 mM KCl. (*d*) Outside-out patch, mean of 25 single channel scans. From a holding potential of 90 mV, a 250 msec-voltage ramp to −110 mV was imposed. Between ramps, the voltage was clamped to 90 mV for 3.25 sec. Standard solutions were used.

KORC using Eq. 6. Arrows indicate the prepulse and the pulse potential, respectively, for the trace shown in *a*, and the corresponding values for *m*, that were inserted into Eq. 2 to fit the activation time course.

Note that Eq. 6 is only valid if the unitary conductance of K^+ channels is voltage independent, i.e. ohmic, over the relevant voltage range. This was the case with 1 mM K^+ in the bath and 120 mM K^+ in the pipette, but not with higher concentrations of K^+ in the bath. Open-channel scans of the current-voltage curve of KORC at different K^+ gradients are shown in Fig. 3. An ohmic behavior was observed with the steep K^+ gradient across the membrane (Fig. 3*a*), but the outward current tended to saturate when the external K^+ concentration was increased (Fig. 3*d*).

An example for the voltage- and K^+ dependence of

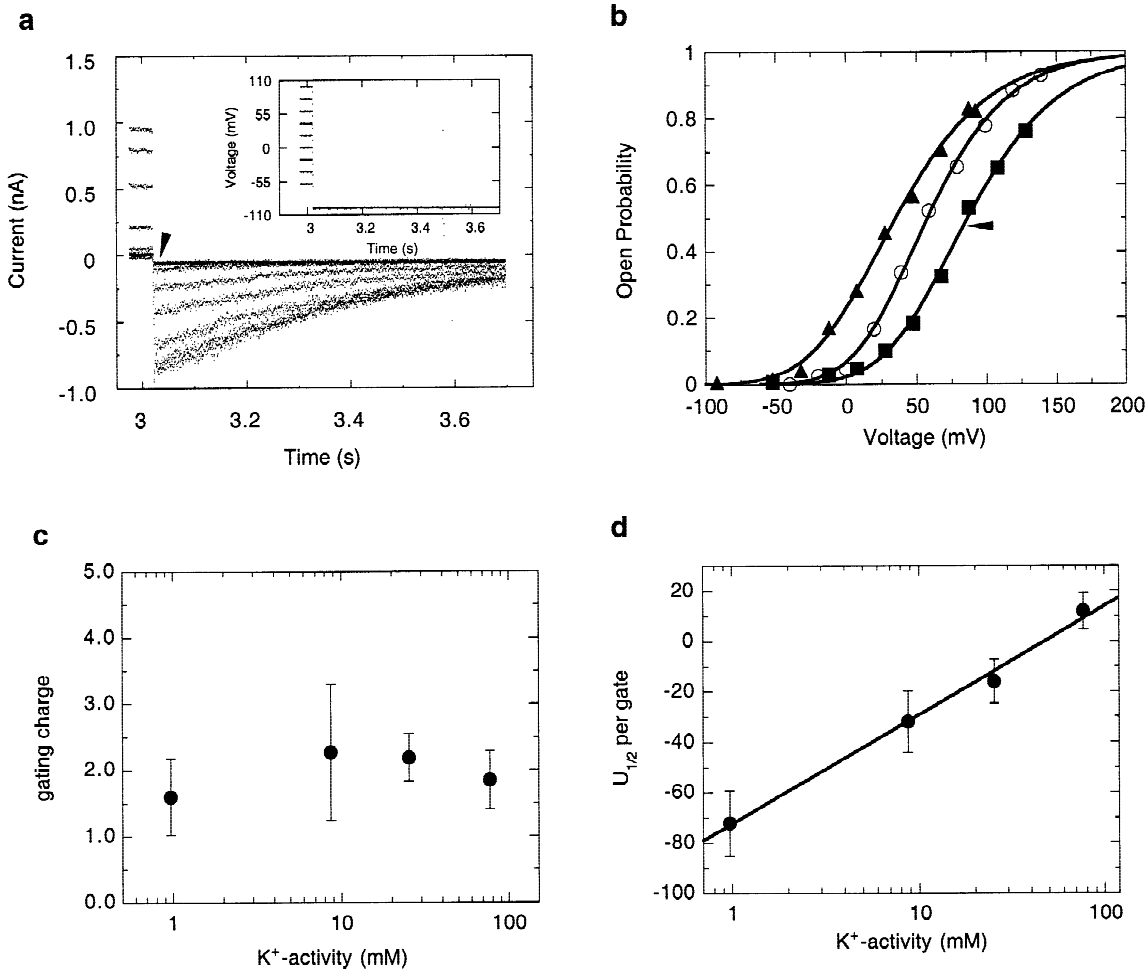

Fig. 4. K^+ and voltage dependence of steady-state KORC currents. (*a*) Relaxations of KORC currents following repolarization to −100 mV (at t = 3.02 sec, *see* inset for the pulse protocol). KORC currents were activated by positive-going voltage steps of 3 sec, ranging from +100 to −20 mV. Tail current amplitudes were measured directly after repolarization (*see* arrow). (*b*) Voltage dependence of KORC open probabilities at 10 (▲), 30 (○) and 100 (■) mM K^+ in the bath (activities: 9/25/77 mM), calculated from tail current amplitudes according to Eq. 5. Data were recorded from one protoplast. Continuous lines indicate Boltzmann fits (Eq. 4). The solutions were composed as follows: *Bath:* 10/30/100 mM KCl, 1 mM $CaCl_2$, 2 mM $MgCl_2$, 10 mM Hepes, pH 5.8 adjusted with MES. *Pipete:* 112 mM K-glutamate, 8 mM KOH, 2 mM HEDTA, 30 μM Ca-gluconate, 2 mM MgATP, 1.75 mM $MgCl_2$ (1.5 μM free Ca^{2+}, mM free Mg^{2+}) pH 7.2, adjusted with BTP. Best fits (10/30/100 mM K^+) were obtained with a midpoint potential ($U_{1/2}$) of −33/−1/19 mV and an apparent minimum gating charge of 1.43/1.67/1.46, respectively. (*c*) Plot of the apparent gating charge as a function of the K^+ activity in the bath. The K^+ activity in the pipette was 91 mM for all experiments. Data were obtained from Boltzmann fits (Eq. 4) of the open probability of KORC in whole cell experiments as shown in Fig. 4*b*. Mean values ± SEM are given for n = 5 (a_{K+} = 1 mM); n = 6 (a_{K+} = 9 mM); n = 6 (a_{K+} = 25 mM); n = 3 (a_{K+} = 77 mM) independent experiments. (*d*) Semilogarithmic plot of the K^+ dependence of midpoint potentials (mean values ± SEM), derived from the same Boltzmann fits. Data were fitted with Eq. 10 (continuous line). For further information, *see* text.

KORC gating as described by Eq. 4 is depicted in Fig. 4*b* for 10, 30 and 100 mM K^+ in the bath (data from one cell). Open probabilities were calculated from current relaxations as shown in Fig. 4*a* using Eq. 5. The Boltzmann curve for the KORC open probability shifted along the voltage axis, depending on the external K^+ concentration. In Fig. 4*c* and *d*, results from Boltzmann fits to a series of experiments with K^+ concentrations in the bath ranging from 1 to 100 mM are summarized. Generally, the steepness of the curves as given by the apparent gating charge did not change significantly with an increase of the K^+ activity in the bath (Fig. 4*c*). K^+ dependence of gating can be explained in the framework of the Hodgkin-Huxley model if closing of the channel depends on binding of K^+ to a site that is exposed to the bath. Transition of the open to the closed state as described by the rate constant β is then given by:

$$\beta = \beta^*[K^+]^n \tag{7}$$

with β* being a scaling factor and n being the Hill coefficient for binding of K^+. The distribution between

open and closed state can be expressed by the following Boltzmann equation that includes a phrase for the K^+ dependence of gating:

$$\frac{m}{1-m} = \exp - \left(\left[U_{1/2,1mMK} - U + \frac{2.303RT}{zF} n \log(a_{K+}) \right] \frac{zF}{RT} \right) \quad (8)$$

And for the open probability of the channel:

$$p_o(U,a_{K+}) = m^4 = \frac{1}{\left[1 + \exp\left\{ \left(U_{1/2,1mMK} - U + \frac{2.303RT}{zF} n \log(a_{K+}) \right) \frac{zF}{RT} \right\} \right]^4} \quad (9)$$

With $U_{1/2,1mMK}$ being the midpoint potential at a concentration of 1 mM K^+ in the bath. When midpoint potentials derived from fits with Eq. 4 are plotted against the K^+ activity in the bath, a semi-logarithmic plot (Fig. 4*d*) renders a linear relationship according to:

$$U_{1/2} = U_{1/2,1mMK} + \frac{2.303RT}{zF} n \log(a_{K+}) \quad (10)$$

For the minimal apparent gating charge *z*, a value of 2 was estimated (Fig. 4*c*). Under these conditions, $U_{1/2,1mMK}$ was extrapolated to −72 mV. The Hill coefficient *n* was determined to be 1.4. The shift in the Boltzmann curve was specific for K^+, adding NMG to the bath did not alter the voltage dependence of the gate (*not shown*).

Using the approach outlined above, the time constant of KORC activation at different K^+ gradients across the plasma membrane could be determined. As shown in Fig. 5, time constants were only slightly voltage dependent. At a given voltage, the rate constants α and β could be calculated from the time constant and the open probability of the gate according to:

$$\alpha = m_\infty/\tau_{act} \quad (11)$$

$$\beta = (1 - m_\infty)/\tau_{act} \quad (12)$$

(Hodgkin & Huxley, 1952). In Fig. 5*b* and *c*, the voltage dependence of α and β, respectively, at different K^+ concentrations in the bath is shown. Note that β shifts with the K^+ concentration in the bath, whereas α is hardly affected by external K^+. In the inset in Fig. 5*c*, β is shown to increase with the external K^+ concentration. These data are in agreement with the model outlined above.

Deactivation of KORC was best described by a single exponential function, with a time constant ranging from 0.3 to 3 sec (Wegner & Raschke, 1994). The Hodgkin-Huxley analysis was not extended to current deactivation, since Vogelzang & Prins (1995) have demonstrated for a K^+ channel very similar to KORC, the outward rectifying K^+ channel in root tissue from *Plantago media*, that rapid flickering strongly affects the deactivation time course. Flickering is independent of the slow gating processes described by the Hodgkin-Huxley model and is most prominent at potentials more negative than E_{K+}. This holds also true for KORC in xylem parenchyma cells from barley roots (Wegner & De Boer, 1997). Rapid closures were also observed at positive potentials but were supposed not to affect the time course of current activation significantly (Schroeder, 1989; Vogelzang & Prins, 1995).

'Sleepy' KORC Channels

For about 50% of the recordings, the Hodgkin-Huxley fit to the KORC activation curves remained poor, especially at strong depolarization. For whole cell recordings, this could have been due to the activation of other depolarization-activated channels with different gating properties. In xylem parenchyma cells, the nonspecific outward rectifier, although downregulated by low levels of cytosolic Ca^{2+} (Wegner & De Boer, 1997), may still be active at extreme depolarization of the membrane (De Boer & Wegner, 1997) and thus forms a potential source of error. Alternatively, deviations from the activation time course as predicted by the Hodgkin-Huxley model could occur in the case of an imperfect voltage clamp of the protoplast. We therefore aimed at a more direct approach to study gating of KORC using averaged single channel recordings (Fig. 6). Repetitive depolarizing voltage steps were applied to inside out patches. The averaged time course of KORC activation was fitted with Eq. 1. An example from an inside out 'macropatch' is shown in Fig. 6*b*. In single sweeps (Fig. 6*a*), discrete current steps of identical size (about 2.3 pA or a multiple of it; *see* inset) were observed. This corresponds to the current amplitude to be expected for KORC under the experimental conditions applied here. Tail currents elicited by a repolarization of the membrane were very noisy, as expected for the 'flickering' gating of KORC when carrying inward currents (*data not shown;* compare Wegner & De Boer, 1997). This would suggest that currents were exclusively carried by KORC channels. About 24 channels were present in this patch. Attempts to fit the entire averaged trace of KORC activation (Fig. 6*b*) with Eq. 1 were unsuccessful (*not shown*). However, an excellent fit of the trace was obtained assuming several 'pools' of channels with identical properties to be activated with a certain time-shift (Fig. 6*b–d*). Here, up to 3 pools could be identified: One pool, consisting of about 17 channels, activated immediately upon depolarization, a second pool of 4 channels activated after a lag-time of about 1.4 sec. The error of the fit for this lag time was 0.02 sec (without taking into account the error

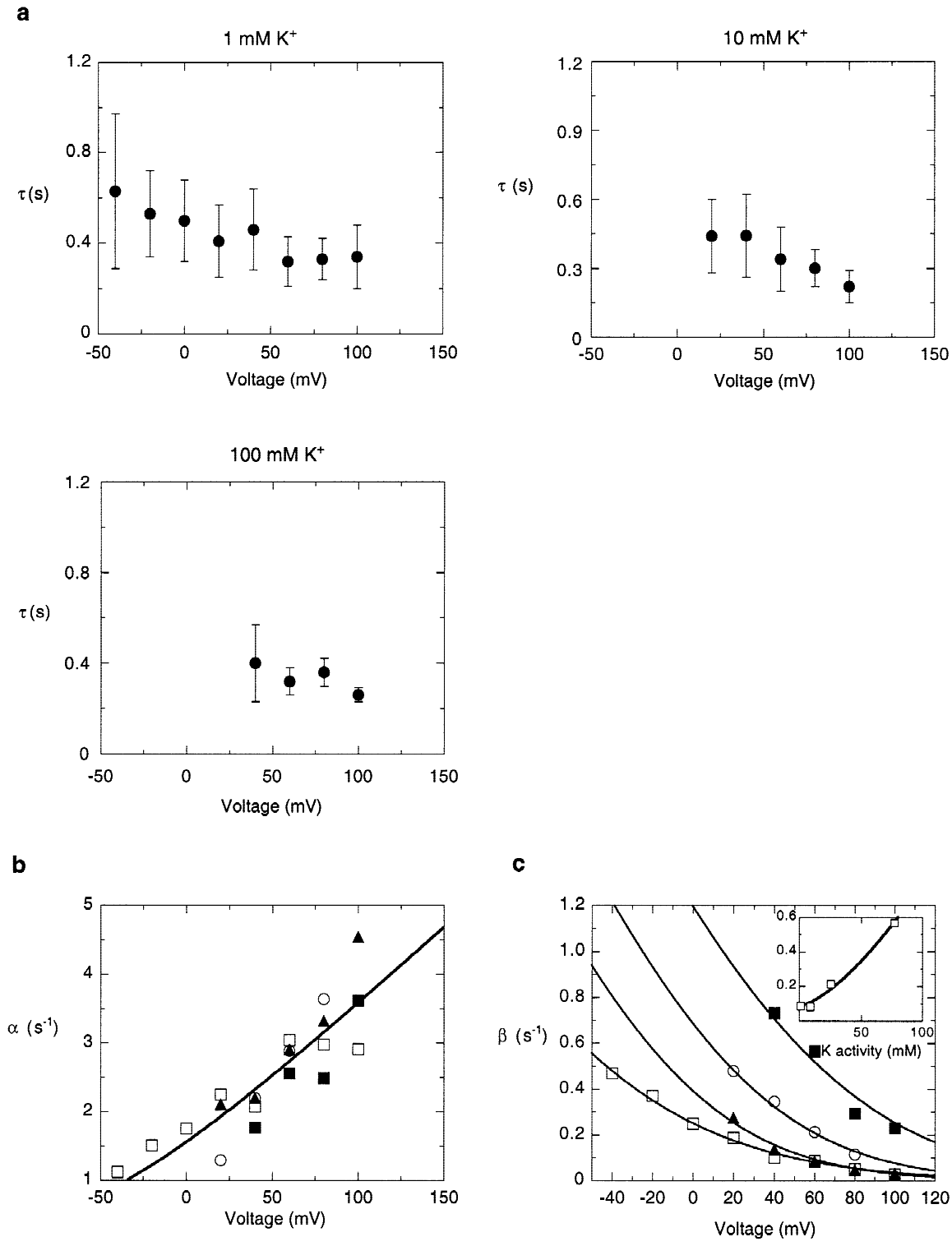

Fig. 5. KORC gating properties. (*a*) Activation time constants obtained from Hodgkin-Huxley fits to KORC activation curves (Eq. 1 or 2, respectively) are plotted against the membrane potential. Mean values of 3–6 experiments ± SD are shown for the following concentrations (activities in brackets) in the bath: 1 (1) mM; 10 (9) mM and 100 (77) mM. (*b*) Voltage dependence of the activation rate constant α, calculated from Eq. 11, for a single gate at K^+ activities of 1 (□), 8 (▲), 25 (○) and 77 (■) mM in the bath. Data were fitted with the equation (Hodgkin & Huxley, 1952): $\alpha = \alpha_o A/[\exp(zFA/RT) - 1]$ and $A = U_\alpha - U$. α_o is a scaling factor, U_α is a parameter describing the voltage dependence of α. The other symbols are explained in the text. Best fit at a gating charge of $z = 2$ rendered a value of −62 mV for $U_\alpha{}^0$ and 0.022 mV^{-1} sec^{-1} for α_o as indicated by the continuous line. (*c*) Voltage dependence, and K^+ dependence (inset), of the deactivation time constant β calculated with Eq. 12 for the same range of external K^+ activities as given in *b*. Data were fitted with the equation $\beta = \beta_o{}^* B\, a_{K+}{}^n/[\exp(zFB/RT) - 1]$, with $B = U - U_\beta$. The Hill coefficient *n* is fixed to 1.4. For the scaling factor $\beta_0{}^*$, a value of 0.018 mV^{-1} sec^{-1} mM^{-1} was obtained for 1 mM K^+ and fixed for the other fits. Best fits (solid lines) were obtained for the factor U_β that indicates the voltage dependence (in brackets K^+ activities in mM): −64 mV (1), −46 mV (9); −37 mV (25), −36 mV (77). Inset: K^+ dependence of β at a membrane voltage of 60 mV.

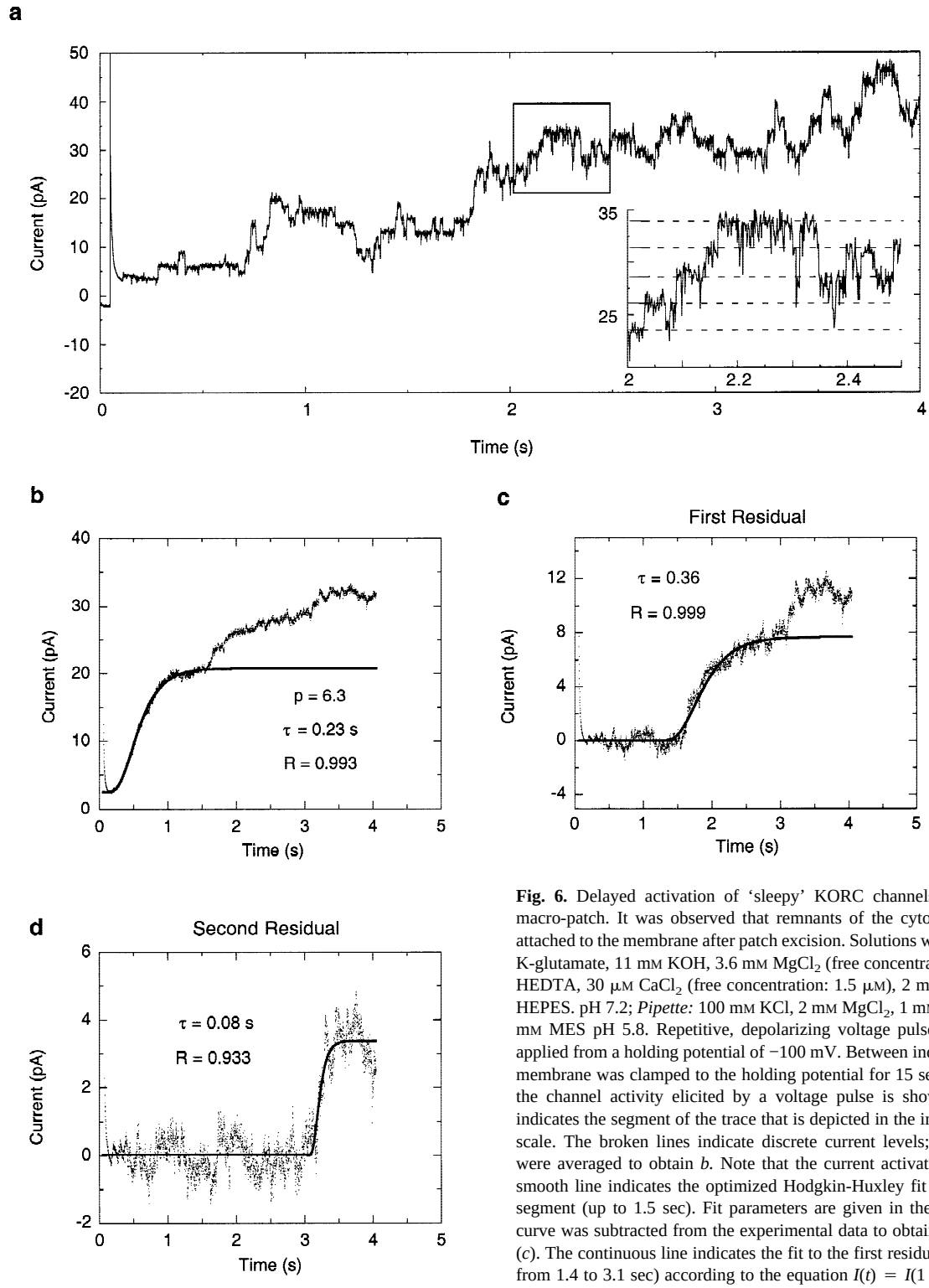

Fig. 6. Delayed activation of 'sleepy' KORC channels in an inside-out macro-patch. It was observed that remnants of the cytoskeleton remained attached to the membrane after patch excision. Solutions were: *Bath:* 239 mM K-glutamate, 11 mM KOH, 3.6 mM $MgCl_2$ (free concentration: 2 mM), 2 mM HEDTA, 30 μM $CaCl_2$ (free concentration: 1.5 μM), 2 mM MgATP, 10 mM HEPES. pH 7.2; *Pipette:* 100 mM KCl, 2 mM $MgCl_2$, 1 mM Ca-gluconate, 10 mM MES pH 5.8. Repetitive, depolarizing voltage pulses to 60 mV were applied from a holding potential of −100 mV. Between individual pulses, the membrane was clamped to the holding potential for 15 sec. An example for the channel activity elicited by a voltage pulse is shown in *a.* The box indicates the segment of the trace that is depicted in the inset on an enlarged scale. The broken lines indicate discrete current levels; 21 single sweeps were averaged to obtain *b.* Note that the current activated 'stepwise.' The smooth line indicates the optimized Hodgkin-Huxley fit (eq. 1) to the first segment (up to 1.5 sec). Fit parameters are given in the figure. The fitted curve was subtracted from the experimental data to obtain the first residual. (*c*). The continuous line indicates the fit to the first residual current (ranging from 1.4 to 3.1 sec) according to the equation $I(t) = I(1 - \exp(-(t - t_{delay})/\tau))^p$ with $t \geq t_{delay}$. t_{delay} is the time at which the 'sleepy' pool started to activate. From the fit, a value of 1.4 sec was determined. The time constant and the regression coefficient are given in the figure. Another current step could be identified by subtracting the calculated curve from the first residual, as shown in *d.* The difference could again well be interpreted in terms of a third pool of channels activating with Hodgkin-Huxley kinetics and an even longer lag phase (3.04 sec).

for calculating the residual). Yet another pool of channels activated with a delay of 3 sec (error 0.003 sec). Conspicuously, one group of 'sleepy' channels activated just when the 'preceding' group was completely activated, resulting in a cascade of sigmoidal-shaped current steps. Similar observations were made in another inside out macropatch with high channel activity. In that patch, one set of about 3 'sleepy' channels manifested itself in addition to about 9 channels responding immediately to a voltage step from −100 to 50 mV (data from 50 repetitive sweeps); the latency for the activation of sleepy channels was about 0.5 sec (*data not shown*). When the same patch was depolarized to 0 mV, no sleepy channels were activated. It should be noted that a 'normal' Hodgkin-Huxley activation time course was observed in other patches with less channel activity (*data not shown*). Several interpretations of these observations are considered in the discussion, and a model for the cooperative interaction of KORC channel pools is presented.

The concept of a stepwise activation of KORC was also successfully applied to those whole cell recordings that could not adequately be described with a 'simple' Hodgkin-Huxley approach (Fig. 7*a–d*). Cascades with up to three pools of 'sleepy' channels could clearly be identified in at least 5 other protoplasts tested. Lag times for the first sleepy pool varied from 0.7 to 1.5 sec. A fixed relationship between 'sleepy' and 'rapid' populations of about 0.2 to 0.3 was often observed (Fig. 7*e*, data from 8 protoplasts). Remarkably, activation of 'sleepy' channels only occurred at a strong depolarization both in averaged single channel traces and whole cell recordings. If less than 70–80% of all gates of the 'rapid' fraction of channels was activated, no "sleepy currents" were observed. In Fig. 8, current-voltage curves of 'rapid' and 'sleepy' channels at different K^+ gradients across the membrane are shown. Note that both curves shift with the external K^+ concentration, consistent with a K^+-dependent gating of all fractions of channels.

KORC Inactivation

In about 5% of the cells challenged with depolarizing voltage steps, KORC was observed to inactivate. An example is shown in Fig. 9*a*. The time course could well be interpreted by introducing a further, independent gating particle (*h*) that causes the channel to inactivate (Hodgkin & Huxley, 1952).

$$I(t) = I_{leak} + I_{max}(1 - \exp(-t/\tau_{act}))^p [h_\infty (h_\infty - 1) \exp(-t/\tau_{inact})] \quad (13)$$

τ_{act} and τ_{inact} are the time constants for activation and for inactivation, respectively; h_∞ is the open probability of the inactivating gate at steady-state conditions.

No pronounced voltage dependence of inactivation was observed (Fig. 9*c*). The time constant τ_{inact} was likewise voltage independent (Fig. 9*b*). Remarkably, in some traces recorded on the same protoplasts, no inactivation occurred (*see* Fig. 9*a* at 30 mV, bottom left). Spontaneous transitions to a noninactivating state were observed in three other protoplasts with partly inactivating KORC. Inactivation of KORC was a rare event that was not predictable. Thus, a more detailed analysis of this phenomenon was precluded.

Discussion

Kinetic Properties of KORC

An outwardly rectifying, K^+ selective channel with a Hodgkin-Huxley type of kinetics has been reported to be present in most higher plant tissues and species investigated so far. Although these K^+ channels appear to have much in common (sigmoidal time course of activation, dependence of gating on the external K^+ concentration a.o.), a detailed analysis of the kinetics has revealed both cell- and species-dependent differences (van Duijn, 1993; Fairley-Grenot & Assmann, 1993). Activation kinetics of the K^+ outward rectifier was best described with two independent gating particles in *Vicia faba* guard cells (Schroeder, 1989), in tobacco suspension cells (van Duijn, 1993), in protoplasts derived from rye roots (White & Lemtiri-Clieh, 1995), and stelar cells from maize (Roberts & Tester, 1995), but with four gating particles in root cells from *Plantago media* (Vogelzang & Prins, 1995). The time constant for current relaxation was only weakly voltage dependent in guard cells and maize stelar cells and displayed an exponential voltage dependence in tobacco suspension cells. Moreover, there is some discussion as to whether the Hodgkin-Huxley model describes the kinetics in guard cell protoplasts adequately. In contrast to Schroeder (1989) and Lemtiri-Clieh (1996), Fairley-Grenot & Assmann (1993) and Ilan, Schwartz & Moran (1994) state that the K^+ outward rectifier in *Vicia faba* guard cells is best described by a sequential kinetic scheme with two closed and one open state, with an activation time course reflected by the sum of two exponential functions. Fairley-Grenot & Assmann state that the situation is different for maize guard cell protoplasts where the Hodgkin-Huxley model (with $p = 3$) was well confirmed. Accordingly, differences were also found for the Boltzmann parameters of the K^+ outward rectifiers (as summarized by Vogelzang & Prins, 1995, Table 2). K^+ outward rectifiers were found to be highly selective for K^+ (in *Plantago media* root cells; Vogelzang & Prins, 1995) or to discriminate weakly among K^+ and Ca^{2+} (in stelar cells, Wegner & De Boer, 1997; Roberts & Tester, 1997). These differences could reflect tissue-specific ex-

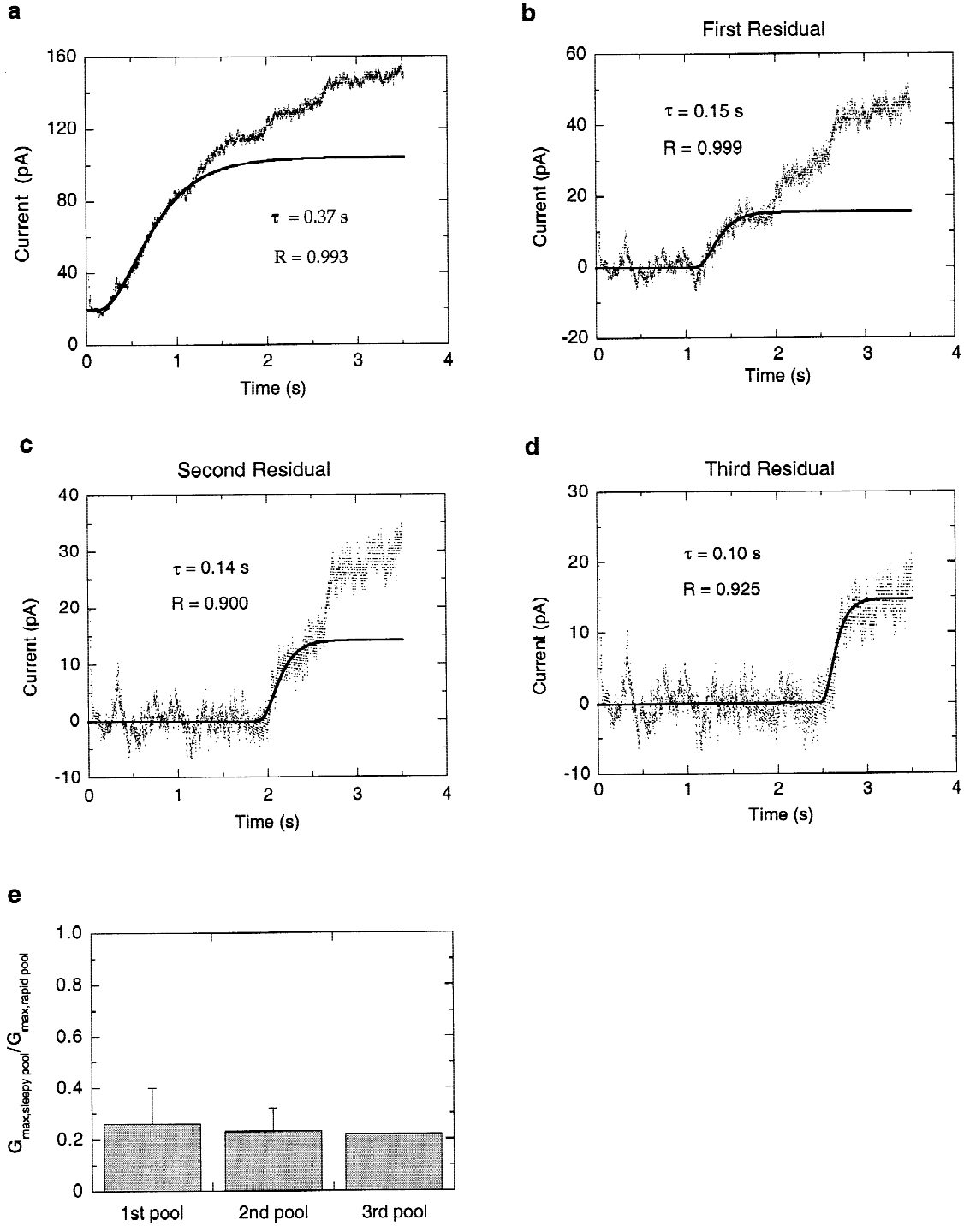

Fig. 7. KORC activation cascade in a whole cell recording. For solutions, *see* legend to Fig. 4 (100 mM K^+ in the bath). In *a*, the current response to a depolarization from −100 to 80 mV is shown. The first segment ranges from the start of the pulse to 1.2 sec. This part of the trace is well fitted by Eq. 1 (continuous line; time constant and regression coefficient for the best fit as indicated in the figure; *p* was fixed to 4). Three residual currents were extracted successively from the experimental data (plots *b, c* and *d*) as described in the legend to Fig. 6, indicating that three 'sleepy' pools were present in the cell. The lag times were (errors for the fit in brackets) 1.08 sec (0.0004 sec; first 'sleepy' pool, (*b*), 1.82 sec (0.01 sec; second 'sleepy' pool, (*c*), 2.46 sec (0.006 sec; third 'sleepy' pool), (*d*). In *e,* the relative size of the 'sleepy' pools compared to the 'rapid pool' is shown (1st pool, average of 6 traces ± SD, 2nd pool, average of 5 traces ± SD, 3rd pool, mean of two traces).

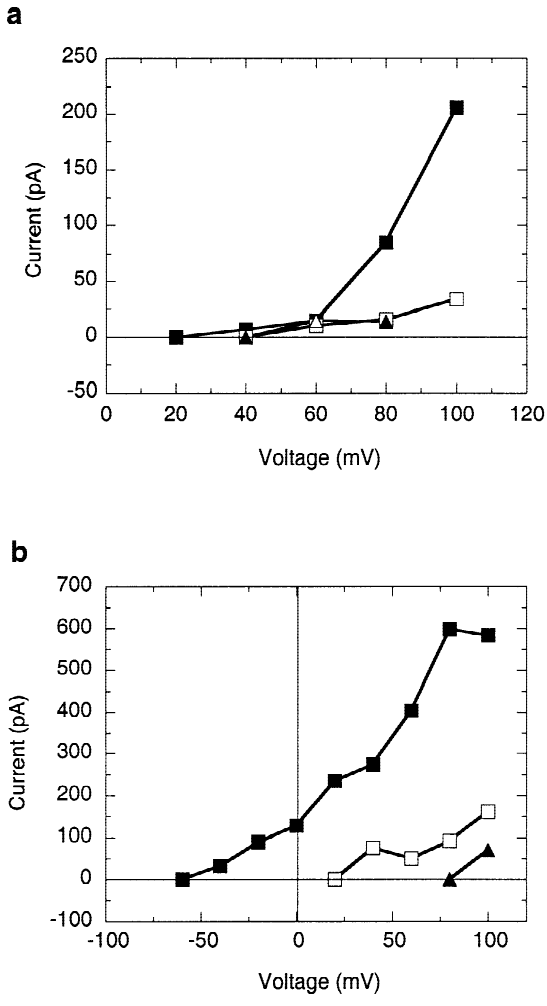

Fig. 8. Current-voltage plots of rapid pool of KORC (■) and first (□), second (▲) and third (Δ), only (*a*) (sleepy pools of KORC at 100 mM K^+ (*a*) and 1 mM K^+ in the bath (*b*)). For *a*, solutions were as described in the legend to Fig. 4. For *b*, standard solutions were used.

pression of genes belonging to one gene family. This was confirmed by the recent discovery of SKOR, a Shaker-like outward rectifying channel that was only expressed in root stelar cells (Gaymard et al., 1998). The latter study also revealed that K^+ outward and inward rectifiers are closely related structurally. So far, no detailed information is available on the kinetic parameters of SKOR from different species expressed in oocytes; a comparison to the data reported here for KORC will be instructive. The model for KORC/SKOR that was described here may be considered as a starting point for further research, including modifications of the protein by site-directed mutagenesis. This kind of work may lead to a more refined and realistic model for gating, as developed for outward rectifiers of the shaker family (e.g., Tytgat & Hess, 1992; Zagotta, Hoshi & Aldrich, 1994; Schoppa & Sigworth, 1998*a* and *b*).

Partial inactivation of KORC observed occasionally (Fig. 9) may result from binding of a small peptide or channel subunit to the mouth of the channel, similar to K^+ channels in animal systems (Hille, 1992). Partial inactivation could be a more general phenomenon of KORC in the intact tissue that is, however, lost in most whole cell recordings, either by protoplast isolation or by dialysis of the cell interior after formation of the whole cell configuration. Alternatively, inactivating outward currents may be carried by a channel different from KORC. This appears to be less likely, though, in view of the fact that inactivation is occasionally lost and restored (Fig. 9*a*). Partial inactivation of a K^+-selective outward rectifier has also been reported for intact guard cells of *Nicotiana benthamania* (Armstrong et al., 1995) and tobacco cell suspension protoplasts (Van Duijn & Flikweert, 1993).

Unfortunately, we have not been able to analyze KORC channel gating in continuous recordings on excised patches since KORC activity could not yet be maintained in a stationary condition for a sufficiently long period. Cooperative interaction of channels and a generally observed rundown in excised patches may contribute to the fluctuations in single channel activity.

Gating of KORC Depends on the External K^+ Concentration

Gating of KORC depended on both voltage and the external K^+ concentration as revealed by a Boltzmann analysis of whole cell steady-state currents (Fig. 4; *see also* Wegner & De Boer, 1997). This is a common feature of K^+ outward rectifiers in higher plant cells, including the one in guard cells (Schroeder, 1988; Blatt 1988), maize stelar cells (Roberts & Tester, 1995) and *Plantago* root cells (Vogelzang & Prins, 1995), and has also been reported for K^+ channels in the rat brain (Pardo et al., 1992). An increase of the external K^+ concentration in the bath leads to a positive shift of the midpoint potential without affecting the steepness of the Boltzmann curve fitted to the open probability (Fig. 4*b–d*). This was shown to reflect the K^+ dependence of the rate constant β for closure of an individual gate (Fig. 5*b* and *c*). Binding of K^+ draws the gate into the closed state, thus counteracting membrane depolarization. The binding site for K^+ appears to be located outside the electrical field of the membrane, suggesting gating to be regulated independently from permeation. A Hill coefficient slightly above 1 may reflect the fact that the K^+ activity in the vicinity of the membrane was higher than the bulk concentration, rather than indicating cooperativity of binding.

Recently, K^+ dependence of outward rectifying K^+ channel gating has been investigated in detail on intact guard cells of *Vicia faba* (Blatt & Gradmann, 1997).

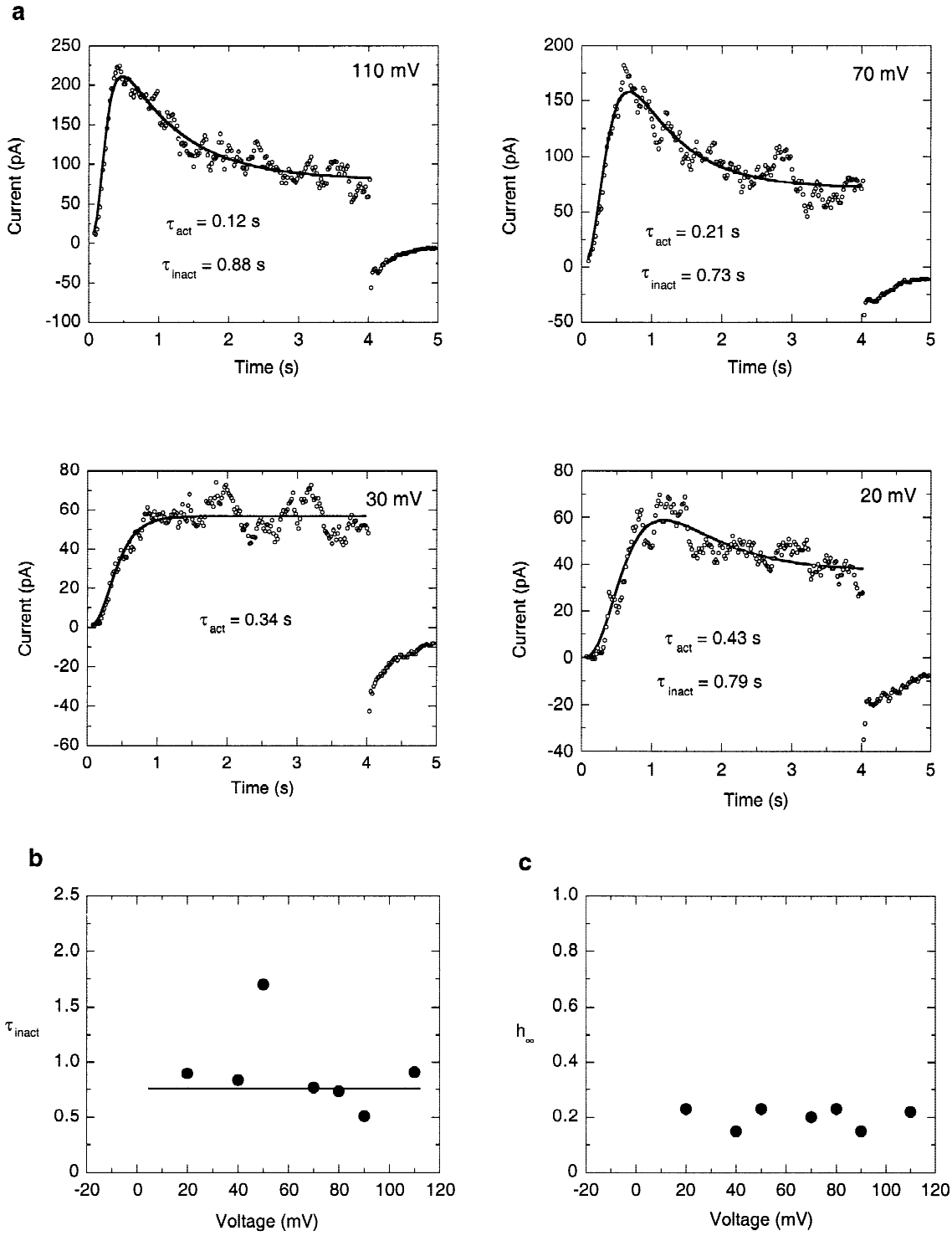

Fig. 9. KORC inactivation. (*a*) Current traces (same cell) at four different conditioning voltages, as indicated in the plots, are shown (between pulses, the membrane was hyperpolarized to −90 mV for 15.5 sec). Each data point (open circle) represents the mean of 20 recorded values. The time course was well described by Eq. 13 (lines calculated from best fits are superimposed on the traces; time constants as given in the figures). Standard solutions, but the pipette medium contained K-glutamate instead of KCl. In *b*, the inactivation time constant, obtained from the fits shown in a, is plotted as a function of the conditioning voltage. It is generally voltage-independent (continuous line). (*c*) Plot of the inactivating variable (h_∞) against the conditioning voltage.

It could be shown that the modulation of the voltage dependence of the channel was not due to a general charge screening, but resulted from a specific interaction of K^+ with the channel protein. Repression of the K^+ conductance of the membrane at any given voltage resulted from the cooperative binding of two K^+ ions to the channel. Blatt and Gradmann (1997) favor a K^+-dependent gating mechanism that is separate from the permeation process. The data could best be described by a sequential model of three closed and one open state; four rate constants depended on the external K^+ concentration.

Apoplastic (external) K^+ does not only affect the open probability, but also the single channel conductance of KORC (Fig. 3). Since the overall membrane conductance is a product of open probability and single-channel conductance, K^+ dependence of the latter will have to be included in a quantitative model of KORC regulation by apoplastic K^+.

Anomalous Gating Properties of KORC: 'Sleepy' KORC Channels

As shown in Figs. 6 and 7, it was obvious from the time course of KORC activation upon a depolarization of the plasma membrane, that several 'sleepy' pools of KORC channels activated with a characteristic delay in part of the experiments. The activation of each pool was well described with a Hodgkin-Huxley formalism, suggesting that gating of channels was independent *within a pool.*

In principle, this can be interpreted in two ways: (i) Populations of 'sleepy' KORC channels activated with a characteristic delay in response to a voltage step. This is an intrinsic property of the channel and does not result from cooperative interaction of the pools. A related phenomenon was recently reported for the delayed rectifier (I_{kr}) in cardiac muscle cells. Co-expression of the gene KvLQT1, encoding for a rapidly activating K^+ channel, with the IsK protein in *Xenopus* oocytes resulted in a dramatic slowdown of the activation kinetics of the channels (Barhanin et al., 1996; Sanguinetti et al., 1996). Similarly, co-assembly of KORC (SKOR) with one or several, yet unidentified subunits could lead to a delay in the response of 'sleepy' channels to a voltage drop. A similar effect was reported for the yeast K^+ channel YKC1. A slowly activating component of the outward current carried by this channel was suppressed by the K^+ concentration in the bath; K^+ sensitivity could be located to single residues at the mouth of the pore by site-directed mutagenesis (Vergani et al., 1998).

(ii) Groups of 'sleepy' channels activate in response to the opening of the preceding, more 'rapid' population. This implies cooperative interaction of several populations of channels. A signal is conveyed from a group of 'rapid' channels, once most of the channels are activated, to one consisting of 'sleepy' channels. Afterwards, the signal is passed from this formerly 'sleepy' group now transformed into a 'rapid' one to another 'sleepy' group. Certainly, this chain of events requires KORC channels to be organized in clusters. Indeed, direct evidence for the existence of K^+ channel clusters comes from a comparison of the number of channels in part of the inside out patches (Fig. 6) with the total number of channels in a whole cell recording. The total number of channels per protoplast can be calculated from the maximal conductance divided by the unitary conductance (Figs. 1 and 7). Up to 24 channels were simultaneously active in the recordings on the excised patch shown in Fig. 6, while 60–400 channels were calculated to be present in one protoplast, i.e., 2.5 to 16 times as many. However, the surface of a xylem parenchyma protoplast is about 50 to 200 times larger than the area of a single patch. [About 1000 μm^2 (Wegner & Raschke, 1994) for a xylem parenchyma protoplast *vs.* 5 to 20 μm^2 for a patch (Sakmann & Neher, 1995)].

One argument in favor of a cooperative gating model is that activation of 'sleepy' channels besides the 'rapid' ones was only observed at strong depolarization (Fig. 8). At these voltages, *m*, the open probability of the gates, was close to unity for both 'rapid' and transformed 'sleepy' populations of KORC channels. This is in agreement with a cooperativity of gating, indicating that almost complete activation of a more 'rapid' pool is required to activate a population of 'sleepy' channels.

A schematic representation of the cooperative model of KORC gating is shown in Fig. 10. Our whole cell and single channel data are in agreement with the assumption that rapid and sleepy channels have identical properties (Fig. 6*a*) and are interconvertible. It is assumed that clusters, once they are in the 'rapid' state, can undergo a transition from a 'tight' to a 'loose' configuration (and *vice versa*), depending on the number of gates per cluster that are in the open state. Transition is assumed to be an all-or-nothing event that requires a certain threshold of active gates. Only in the 'loose' configuration the cluster is able to force neighboring 'sleepy' clusters into the 'rapid' state (Fig. 10*a*), thus leading to a feedforward-effect of channel activation. A cartoon illustrating the chain of events is shown in Fig. 10*b*. Note that 'rapid' clusters should activate neighboring 'sleepy' clusters within a critical distance. Thus, a propagation of the signal is achieved, leading to a cascade of current activation.

So far, we can only speculate on the mechanism that could transform 'tight' into 'loose' clusters. One possibility is that opening of KORC channel gates leads to a charge separation in the protein due to the movement of gating charges. Transition from the 'tight' to a 'loose' cluster may, in fact, be brought about by electrostatic forces: Charge separation leads to a local dipole moment

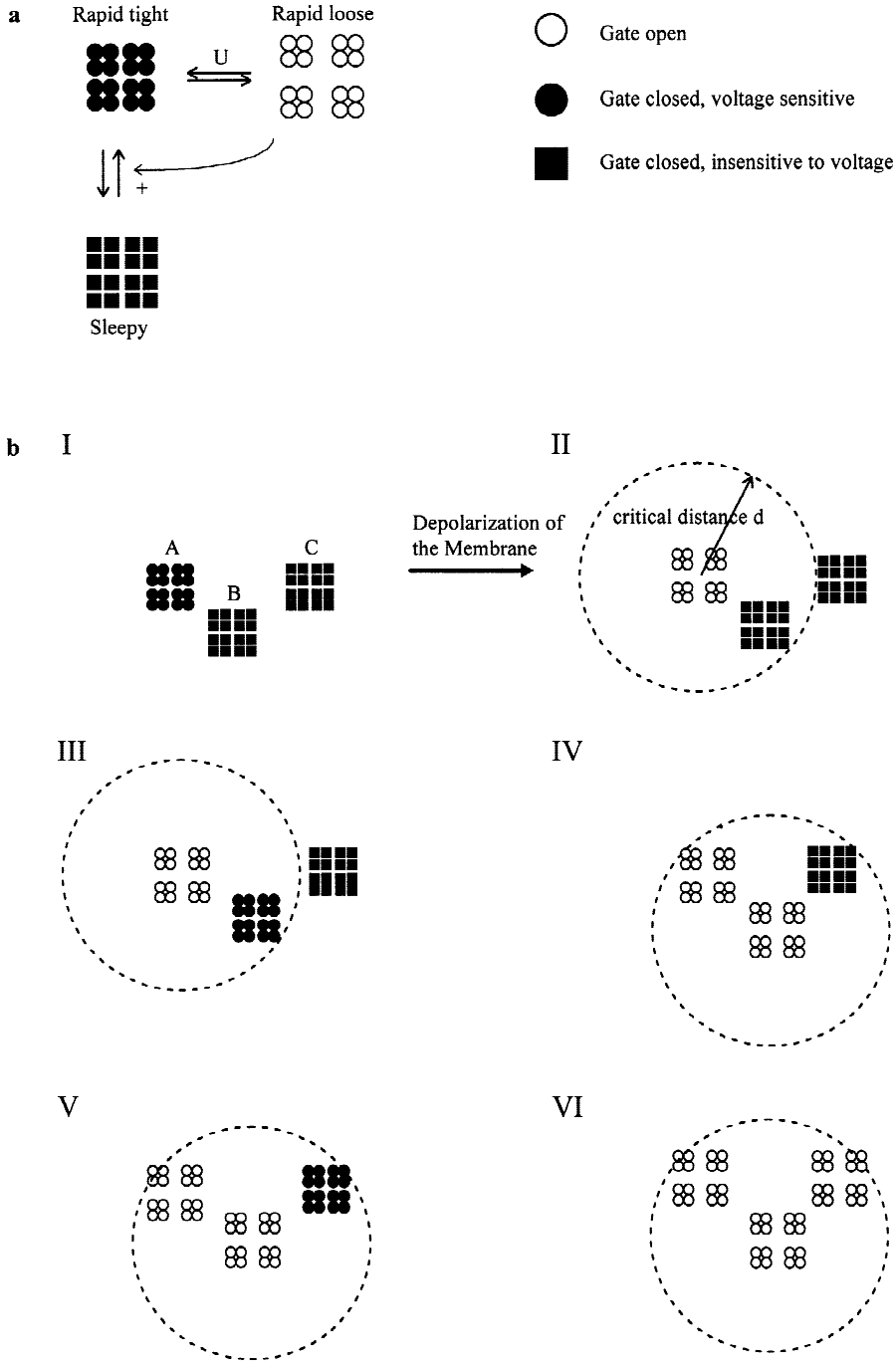

Fig. 10. Cartoons illustrating a possible gating mechanism of KORC clusters. Different symbols are used for gates being either in the closed and voltage-insensitive, in the closed and voltage-sensitive or in the open state. One channel comprises four gates. For simplicity, all clusters are supposed to be homogeneous with respect to the state of the channels. Also, a constant number of four channels per cluster is assumed arbitrarily. (*a*) Reaction scheme of KORC channel clusters that switch between three different states ('sleepy', 'rapid tight' and 'rapid loose'). In the 'rapid loose' configuration, a cluster strongly increases the probability of neighboring 'sleepy' clusters to achieve the 'rapid tight' configuration, as indicated by the arrow. (*b*) Possible chain of events in an activation cascade of KORC channels upon a depolarization of the plasma membrane of xylem parenchyma cells. At a hyperpolarized state of the membrane, channels are closed and clusters reside either in the 'sleepy' or in the 'rapid tight' configuration. Membrane depolarization leads to an opening of voltage-sensitive channels in 'rapid tight' clusters (like A) and, in turn, to a transition of the cluster into the 'rapid loose' state (step I to II). Consequently, 'sleepy' clusters within a critical distance (like B) switch to the 'rapid tight' state (picture III), and channels belonging to this cluster open likewise. Now the sequence of events is repeated: Complete activation of the channels is correlated with a transition to the 'rapid loose' state of cluster B (picture IV), and cluster C is triggered and transferred into the 'rapid loose' state as well (pictures V, VI). This scenario would lead to a "three-step-cascade" of KORC activation kinetics.

in the channel protein, resulting in a conformational change. If the charges are exposed, mutual repulsion of channels may destabilize tightly packed clusters (as was tacitly implied by the terms 'tight' and 'loose'). If the polarization exceeds a critical threshold, mutual electrostatic repulsion of proteins may cause a transformation of tight clusters to loose aggregations of channels. A signal propagating mechanically in the lipid phase may trigger nearby 'sleepy' clusters, turning them into 'rapid' ones.

The fact that 'sleepy' channels were not observed in all whole cell and averaged single channel recordings may indicate that the intricate structure of KORC channel assembly was not conserved in all protoplasts, perhaps depending on the intactness of the cytoskeleton. Remarkably, the number of 'sleepy' pools could vary in successive depolarizing sweeps imposed on the same protoplast (*not shown*). This may be due to a variable distance of clusters floating in the membrane. It may also reflect the fact that the number of 'sleepy' clusters could not always be properly resolved from the time course of KORC activation.

A cooperative behavior of K^+ channels in a plant system was previously reported for cytoplasmic droplets from *Chara corallina* (Draber, Schultze & Hansen, 1993). Draber et al. investigated channel activity in continuous recordings using the inside-out configuration. A quantitative analysis revealed cooperative mode-shifting, i.e., the simultaneous transition of several channels from one gating mode to another. This effect bears some similarity with the observation reported here; especially, Draber et al. (1993) suggest channels to be organized in clusters of uniform gating mode. Likewise, they suggest a mechanical interaction of neighboring channels. Evidence for a clustering of channels was also recently reported for anion channels in the plasma membrane of *Chara corallina* (McCulloch, Laver & Walker, 1997).

What should be the physiological benefit for the cell to activate still more channels at a strong depolarization of the membrane? Voltage-independent recruitment of channels of the KORC type in guard cells has been reported, e.g., in connection with temperature changes (Ilan, Moran & Schwartz, 1995) or phosphorylation (Thiel & Blatt, 1994). While the putative physiological role of the complex gating mechanism of KORC remains obscure, it is obvious that ignoring it in the quantitative analysis of whole cell currents would lead to serious errors in the estimation of the kinetic parameters of the channel.

Implications of a Kinetic Analysis of the Main Ionic Conductances of Xylem Parenchyma Cells for Understanding the Physiology of Salt Transport into the Xylem

Salt release by xylem parenchyma cells is supposed to be mediated by the simultaneous activity of cation and anion channels (Wegner & Raschke, 1994; Wegner & De Boer, 1997; Roberts & Tester, 1995). Thermodynamically, salt release is confined to membrane potentials more positive than the Nernst potential of potassium.

From the membrane conductance for an ion at a given voltage, the flux across the membrane can be calculated according to:

$$J^i_{CX} = \frac{\overline{G}_i(U) \cdot (U - E_{rev}) \cdot A}{z_i \cdot F} \tag{14}$$

J^i_{cx} is the flux of an ion from the symplast into the xylem, $\overline{G}_i(U)$ is the chord conductance of an ion per surface area of the membrane, A is the effective membrane area per length of the root involved in the release of salts, z_i and F have their usual meaning. So, by solving Eq. 14, ion fluxes between the symplast and the apoplast of the root can be calculated. It is obvious that a knowledge of the voltage dependence of the K^+ conductance leading to K^+ efflux from xylem parenchyma cells is crucial for a quantitative treatment of salt release into the root xylem. Currently, a quantitative description of the voltage dependence of KORC, as presented in this paper, as well as of the K^+ inward rectifier(s) KIRC (Wegner, De Boer & Raschke, 1994) are available. A quantitative analysis of anion currents and the proton pump will have to follow. This is an approach for modelling salt export from the root to the shoot. It should be noted that regulation of the conductances by factors other than the membrane potential and the K^+ concentration in the xylem, e.g., the cytosolic Ca^{2+} concentration, have to be included in a comprehensive model. Recently, the contribution of salt recirculated by the phloem has been emphasized (Marschner, Kirkby & Engels, 1997; Wegner & De Boer, 1997). Moreover, salt transport into the xylem cannot be considered independently from radial movement of water, and a possible influence of pressure gradients on salt transport has to be taken into account.

The authors wish to thank Dr. Sake Vogelzang and Mr. Paul Giesberg, Amsterdam, The Netherlands, for many helpful suggestions and critical reading of an earlier version of the manuscript, Drs. Hervé Sentenac and Jean-Baptiste Thibaud, Montpellier, France, for suggestions on the manuscript and for making unpublished data available to us and Drs. T. Bayerl and U. Zimmermann, Würzburg, Germany, for providing computer facilities. LHW was supported by a grant from the Studienstiftung des Deutschen Volkes.

References

Armstrong, C.M. 1969. Inactivation of the potassium conductance and related phenomena caused by quarternary ammonium ion injection in squid axons. *J. Gen. Physiol.* **54:**553–575

Armstrong, C.M. 1975. K^+ pores of nerve and muscle membranes. *In:* Membranes-A Series of Advances. Vol. 3. G. Eisenman, editor. pp. 325–358. New York

Armstrong, F., Leung, J., Grabov, A., Brearley, J., Giraudat, J., Blatt, M.R. 1995. Sensitivity to absisic acid of guard-cell K^+ channels is

suppressed by abil-1, a mutant *Arabidopsis* gene encoding a putative protein phosphatase. *Proc. Natl. Acad. Sci. USA* **92:**9520–9524

Barhanin, J., Lesage, F., Guillemare, E., Fink, M., Lazdunski, M., Romey, G. 1996. KvLQT1 and IsK (minK) proteins associate to form the IKS cardiac potassium current. *Nature* **384:**78–80

Blatt, M.R. 1988. Potassium-dependent, bipolar gating of K^+ channels in guard cells. *J. Membrane Biol.* **102:**235–246

Blatt, M.R., Gradmann, D. 1997. K^+-sensitive gating of the K^+ outward rectifier in *Vicia* guard cells. *J. Membrane Biol.* **158:**241–256

De Boer, A.H., Wegner, L.H. 1997. Regulatory mechanisms of ion channels in xylem parenchyma cells. *J. Exp. Bot.* **48:**441–449

Draber, S., Schultze, R., Hansen, U.P. 1993. Cooperative behaviour of K^+ channels in the tonoplast of *Chara corallina*. *Biophys. J.* **65:**1553–1559

Drew, M.C., Webb, J., Saker, L.R. 1990. Regulation of K^+ uptake and transport to the xylem in barley roots; K^+ distribution determined by electron probe X-ray microanalysis of frozen-hydrated cells. *J. Exp. Bot.* **41:**815–825

Fairley-Grenot, K.A., Assmann, S.M. 1993. Comparison of K^+ channel activation and deactivation in guard cells from a dicotyledon (*Vicia faba* L.) and a graminadeous monocotyledon (*Zea mays*). *Planta* **189:**410–419

Gaymard, F., Pilot, G., Lacombe, B., Bouchez, D., Bruneau, D., Boucherez, J., Michaux-Ferrière, N.M., Thibaud, J.-B., Sentenac, H. 1998. Identification and disruption of a plant Shaker-like outward channel involved in K^+ release into the xylem sap. *The Cell* **94:**647–655

Hille, B. 1992. Ionic Channels of Excitable Membranes. Sinauer, Sunderland, MA

Hodgkin, A.L., Huxley, A.F. 1952. A quantitative description of membrane current and its application to conduction and excitation in nerves. *J. Physiol.* **117:**500–544

Ilan, N., Moran, N., Schwartz, A. 1995. The role of potassium channels in the temperature control of stomatal aperture. *Plant Physiol.* **108:**1161–1170

Ilan, N., Schwartz, A., Moran, N. 1994. External pH effects on the depolarization-activated K channels in guard cell protoplasts of *Vicia faba*. *J. Gen. Physiol.* **103:**807–831.

Kolb, H.-A., Marten, I., Hedrich, R. 1995. Hodgkin-Huxley analysis of a GCAC1 anion channel in the plasma membrane of guard cells. *J. Membrane Biol.* **146:**273–282

Lemtiri-Clieh, F. 1996. Effects of internal K^+ and ABA on the voltage-dependence of the outward K^+ rectifier in *Vicia* guard cells. *J. Membrane Biol.* **153:**105–116

Marschner, H., Kirkby, E.A., Engels, C. 1997. Importance of cycling and recycling of mineral nutrients within plants for growth and development. *Botanica Acta* **110:**265–273

McCulloch, S.R., Laver, D.R., Walker, N.A. 1997. Anion channel activity in the *Chara* plasma membrane: cooperative subunit phenomena and a model. *J. Exp. Bot.* **48:**383–397

Pardo, L.A., Heinemann, S.H., Teralu, H., Ludewig, U., Lorra, C., Pongs, O., Stühmer, W. 1992. Extracellular K^+ specifically modulates a rat brain K^+ channel. *Proc. Natl. Acad. Sci. USA* **89:**2466–2470

Roberts, S.K. 1998. Regulation of K^+ channels in maize roots by water stress and abscisic acid. *Plant Physiol.* **116:**145–153

Roberts, S.K., Tester, M. 1995. Inward and outward K^+-selective currents in the plasma membrane of protoplasts from maize root cortex and stele. *The Plant Journal* **8:**101–115

Roberts, S.K., Tester, M. 1997. Permeation of Ca^{2+} and monovalent cations through an outwardly rectifying channel in maize root stelar cells. *J. Exp. Bot.* **48:**839–846

Sakmann, B., Neher, E. 1995. Geometric parameters of pipettes and membrane patches. *In:* Single Channel Recording. B. Sakmann and E. Neher, editors. p. 637. 2nd edition. Plenum Press, New York and London

Sanguinetti, M.C., Currant, M.E., Zou, A., Shen, J., Spector, P.S., Atkinson, D.L., Keating, M.T. 1996. Coassembly of KvLQT1 and minK (IsK) proteins to form cardiac I_{KS} potassium channel. *Nature* **384:**80–83

Schoppa, N.E., Sigworth, F.J. 1998*a*. Activation of *Shaker* potassium channels. I Characterization of voltage-dependent transitions. *J. Gen. Physiol.* **111:**271–294

Schoppa, N.E., Sigworth, F.J. 1998*b*. Activation of *Shaker* potassium channels. III An activation gating model for wild-type and V2 mutant channels. *J. Gen. Physiol.* **111:**313–342

Schroeder, J.I. 1988. K^+ transport properties of K^+ channels in the plasma membrane of *Vicia faba* guard cells. *J. Gen. Physiol.* **92:**667–683

Schroeder, J.I. 1989. Quantitative analysis of outward rectifying K^+ channel currents in guard cell protoplasts from *Vicia faba*. *J. Membrane Biol.* **107:**229–235

Thiel, G., Blatt, M.R. 1994. Phosphatase antagonist okadaic acid inhibits steady-state K^+ currents in guard cells of *Vicia faba*. *Plant J.* **5:**727–733

Tytgat, J., Hess, P. 1992. Evidence for cooperative interactions in potassium channel gating. *Nature* **359:**420–423

Van Duijn, B. 1993. Hodgkin-Huxley analysis of whole-cell outward rectifying K^+ currens in protoplasts from tobacco cell suspension cultures. *J. Membrane Biol.* **132:**77–85

Van Duijn, B., Flikweert, M.T. 1993. Ionic channels in tobacco cell suspension protoplasts at different days of culturing. Abstractbook SEB Symposium: Membrane Transport in Plants and Fungi: Molecular Mechanisms and Control

Vergani, P., Hamilton, D., Jarvis, S., Blatt, M.R. 1998. Mutations in the pore regions of the yeast K^+ channel YKC1 affect gating by extracellular K^+. *EMBO J.* **17:**7190–7198

Vogelzang, S.A., Prins, H.B.A. 1995. Kinetic analysis of two simultaneously activated K^+ currents in roots cell protoplasts of *Plantago media*. *J. Membrane Biol.* **146:**113–122

Wegner, L.H., De Boer, A.H. 1996. Dynamics of outward rectifying currents in xylem parenchyma cells from barley roots. *In:* The Role of Ion Channels in Salt Transport Between the Xylem and Adjacent Cells. PhD thesis, Vrije Universiteit, Amsterdam

Wegner, L.H., De Boer, A.H. 1997*a*. Properties of two outward-rectifying channels in root xylem parenchyma cells suggest a role in K^+ homeostasis and long-distance signaling. *Plant Physiol.* **115:**1707–1719

Wegner, L.H., De Boer, A.H. 1997*b*. Two inward K^+ channels in the xylem parenchyma of barley roots are regulated by G-protein modulators through a membrane-delimited pathway. *Planta* **203:**506–516

Wegner, L.H., De Boer, A.H., Raschke, K. 1994. Properties of the K^+ inward rectifier in the plasma membrane of xylem parenchyma cells from barley roots: Effects of TEA^+, Ca^{2+}, Ba^{2+}, and La^{3+}. *J. Membrane Biol.* **142:**363–379

Wegner, L.H., Raschke, K. 1994. Ion channels in the xylem parenchyma of barley roots. *Plant Physiol.* **105:**799–813

White, P.J., Lemtiri-Clieh, F. 1995. Potassium currents across the plasma membrane of protoplasts derived from barley roots: a patch clamp study. *J. Exp. Bot.* **46:**497–511

Zagotta, W.N., Hoshi, T., Aldrich, R.W. 1994. Shaker potassium channel gating. III. Evaluation of kinetic models for activation. *J. Gen. Physiol.* **103:**321–362